Am J Physiol Gastrointest Liver Physiol 299: G136–G143, 2010.
First published April 29, 2010; doi:10.1152/ajpgi.00014.2010.

The apical (hPepT1) and basolateral peptide transport systems of Caco-2 cells are regulated by AMP-activated protein kinase

Myrtani Pieri,[1,2] Helen C. Christian,[2] Robert J. Wilkins,[2] C. A. R. Boyd,[2] and David Meredith[1,2]

[1]*School of Life Sciences, Oxford Brookes University, Headington, Oxford;* [2]*Department of Physiology, Anatomy and Genetics, University of Oxford, Oxford, United Kingdom*

Submitted 20 January 2010; accepted in final form 23 April 2010

Pieri M, Christian HC, Wilkins RJ, Boyd CAR, Meredith D. The apical (hPepT1) and basolateral peptide transport systems of Caco-2 cells are regulated by AMP-activated protein kinase. *Am J Physiol Gastrointest Liver Physiol* 299: G136–G143, 2010. First published April 29, 2010; doi:10.1152/ajpgi.00014.2010.—The effect of 5-aminoimidazole-4-carboxamide-ribonucleoside (AICAR) activation of the AMP-activated protein kinase (AMPK) on the transport of the model radiolabeled dipeptide [^{3}H]-D-Phe-L-Gln was investigated in the human epithelial colon cancer cell line Caco-2. Uptake and transepithelial fluxes of [^{3}H]-D-Phe-L-Gln were carried out in differentiated Caco-2 cell monolayers, and hPepT1 and glucose transporter 2 (GLUT2) protein levels were quantified by immunogold electron microscopy. AICAR treatment of Caco-2 cells significantly inhibited apical [^{3}H]-D-Phe-L-Gln uptake, matched by a decrease in brush-border membrane hPepT1 protein but with a concomitant increase in the facilitated glucose transporter GLUT2. A restructuring of the apical brush-border membrane was seen by electron microscopy. The hPepT1-mediated transepithelial (A-to-B) peptide flux across the Caco-2 monolayers showed no significant alteration in AICAR-treated cells. The electrical resistance in the AICAR-treated monolayers was significantly higher compared with control cells. Inhibition of the sodium/hydrogen exchanger 3 (NHE3) had an additive effect to AICAR, suggesting that the AMPK effect is not via NHE3. Fluorescence measurement of intracellular pH showed no reduction in the proton gradient driving PepT1-mediated apical uptake. The reduction in apical hPepT1 protein and dipeptide uptake after AICAR treatment in Caco-2 cells demonstrates a regulatory effect of AMPK on hPepT1, along with an influence on both the microvilli and tight junction structures. The absence of an associated reduction in transepithelial peptide movement implies an additional stimulatory effect of AICAR on the basolateral peptide transport system in these cells. These results provide a link between the hPepT1 transporter and the metabolic state of this model enterocyte.

SLC15a1; 5-aminoimidazole-4-carboxamine ribonucleoside; glucose transporter 2; intestinal epithelium; membrane transport

TRANSPORT OF PROTEIN IN THE FORM of small peptides (di-/tripeptides) is the principal route of dietary protein absorption. The H^+-coupled di- and tripeptide transporter, PepT1, plays a key role in this process. PepT1, which is located in the apical membrane of certain epithelial cells, is a protein that uses the proton electrochemical gradient as the driving force to transport di- and tripeptides into the cell (5). In the case of nonhydrolyzable peptides, an as yet molecularly unidentified basolateral peptide transporter operates in series to allow transepithelial uptake (25). The acid-loading activity of PepT1 in intestinal epithelial cells requires the sodium/hydrogen exchanger 3 (NHE3) isoform of the Na^+-proton antiporter in the apical membrane for the recovery of the cell from the acid load (18). NHE3 exports protons, entering the cell via PepT1, in exchange for extracellular Na^+ ions. This system is coupled to energy consumption through the function of the basolateral Na/K-ATPase, which exports Na^+ ions out of the cell with the consumption of ATP. Peptide absorption therefore requires an input of cellular metabolic energy.

To investigate the properties of intestinal peptide transport, the human intestinal cell line Caco-2 was employed. Caco-2 cells have been extensively used over the last twenty years as a model of the intestinal barrier. The parental cell line, originally obtained from a human colon adenocarcinoma, undergoes a process of spontaneous differentiation in culture that leads to the formation of a monolayer of polarized cells, expressing morphological and functional characteristics of the mature small intestinal enterocyte (13). Confluent monolayers form tight junctions between cells and exhibit the dome formation and electrical properties of the epithelium (27). Both human PepT1 (hPepT1, Ref. 7) and the basolateral peptide transporter have been shown to be functionally present in the appropriate membrane of Caco-2 cells (7, 25, respectively).

The AMP-activated protein kinase (AMPK) has recently emerged as a regulator of membrane transport proteins, which may permit sensitive transport-metabolism crosstalk (9). Nutrient transporters have also been shown to be under AMPK regulation (8). The pharmacological activation of AMPK is possible through the use of 5-aminoimidazole-4-carboxamine ribonucleoside (AICAR). AICAR is rapidly transported into cells, probably by the adenosine transporter (30), and phosphorylated to form the AMP mimetic 5-aminoimidazole-4-carboxamine ribonucleoside monophosphate, which directly activates AMPK. AICAR has been shown to activate AMPK without disturbing the cellular concentration of ATP or its metabolites, ADP or AMP, and has thus been widely used for specific activation of AMPK (4).

The aim of the present study was to use these tools to investigate whether the proton-coupled peptide transporter hPepT1 is linked to the metabolic state of the epithelial cell; more specifically, it was to determine the effect of AICAR on the transport of the model radiolabeled dipeptide [^{3}H]-D-Phe-L-Gln by hPepT1 in Caco-2 cells.

MATERIALS AND METHODS

Materials. AICAR was purchased from Sigma-Aldrich (Poole, UK). [^{3}H]-D-Phe-L-Gln (17.4 Ci/mmol) was custom-synthesized by Cambridge Research Biochemicals (Stockton-on-Tees, UK). Tissue Culture Medium (EMEM) was purchased from LGC-Promochem (Teddington, Middlesex, UK). Fetal calf serum (FCS) was purchased

Current address of M. Pieri: Dept. of Biological Sciences, University of Cyprus, 1678, Nicosia, Cyprus.

Address for reprint requests and other correspondence: D. Meredith, School of Life Sciences, Oxford Brookes Univ., Headington, Oxford OX3 0BP, UK (e-mail: dmeredith@brookes.ac.uk)

from GIBCO (Invitrogen, Grand Island, NY), and penicillin-streptomycin 1% (vol/vol) was purchased from Sigma-Aldrich. Trypsin-EDTA (0.25% wt/vol and 0.53 mM, respectively) was purchased from LGC-Promochem. PBS was purchased from GIBCO. Cell culture supplies were purchased from Corning and Falcon. All other chemicals were purchased from Sigma-Aldrich, unless specified.

Cell culture. The Caco-2 cell line was obtained from American Type Culture Collection (Rockville, MD). Cells were grown routinely on 75-cm^2 plastic culture flasks (Falcon) in EMEM supplemented with 10% (vol/vol) FCS and 1% (vol/vol) penicillin-streptomycin at 37°C in an atmosphere of 5% CO_2 and 90% relative humidity. The medium was replaced every 2–3 days after incubation. Cells were passaged, 1:5, approximately every 5 days (at 70–80% confluence) using 0.25% wt/vol Trypsin-0.53 mM EDTA. The cells were not tested for mycoplasm contamination.

Caco-2 cell uptake studies. Caco-2 cells were cultured in six-well plates for 10 days after the formation of a complete monolayer of cells to allow differentiation, with medium replacement every 2 days. Cells were divided into two groups, and cells in the first group were treated with 1 mM AICAR (in EMEM) for 24 h before uptake experiments. On the day of the experiment, cell monolayers were washed three times with Krebs solution (pH 5.5, 37°C), and then 500 μl Krebs (pH 5.5) plus 0.42 μM [^{3}H]-D-Phe-L-Gln was added to each of the wells. Half of the wells for cells under each condition (i.e., control or AICAR-treated) had an additional 20 mM Gly-L-Gln. Cells were incubated at 37°C for 1 h. At the end of the incubation period, cell monolayers were washed three times with fresh cold Krebs (pH 7.4) to remove extracellular [^{3}H]-D-Phe-L-Gln. Intracellular peptide was determined by scintillation counting after the cells were lysed with 500 μl of 1% NaOH/0.1% SDS. The PepT1-mediated transport of [^{3}H]-D-Phe-L-Gln into the Caco-2 cells was calculated by subtraction of the transport in the presence of 20 mM Gly-L-Gln from that measured in its absence. Gly-L-Gln is a well-characterized PepT1 substrate with a K_i against [^{3}H]-D-Phe-L-Gln uptake of approximately 0.2 mM at pH 5.5 (20).

The protein content of cells, control and AICAR-treated, was determined by a colorimetric assay. Briefly, after the 1-h incubation, cells were washed and lysed with 500 μl of 1% NaOH/0.1% SDS for 24 h, and total cellular protein was determined using DC Protein Assay Reagent (Bio-Rad, Hercules, CA) following the manufacturer's instructions.

Western blotting. Confluent monolayers of Caco-2 cells grown on solid plastic were treated for 24 h with 1 mM AICAR (with untreated cells as a control) before lysing in RIPA buffer with protease and phosphatase inhibitors (both at 1%). Samples were run on a 10% SDS-PAGE gel, transferred overnight onto nitrocellulose (Whatman, Kent, UK) and blocked with 5% milk in (TBST) (1 h). The membrane was probed with anti-phospho-Ser79-acetyl-CoA-carboxylase (Cell Signaling Technologies, Beverly, MA; 1:200 in 5% BSA TBST, overnight) or anti-α-tubulin as a loading control (Sigma) followed by the appropriate horseradish peroxidase-conjugated secondary (Jackson ImmunoResearch, Suffolk, UK; 1:2,000, 5% milk TBST, 1 h). The blot was visualized with chemiluminescence (ECL, GE Healthcare Life Sciences, Buckinghamshire, UK).

Transwell transport studies. For Transwell transport studies, Caco-2 cells (passages between 32 and 45) were seeded on polyester filters (0.4-μm pores, 0.3-cm^2 growth area) in the Transwell Cell Culture Chamber System (Costar, Appleton Woods, Birmingham, UK) at a density of 5×10^5 cells/filter, as described previously (27). The cell monolayers were cultured with 200 μl and 600 μl of complete EMEM in the apical and the basolateral compartment, respectively.

To assess the integrity of the monolayer, transepithelial electrical resistance (TEER) was monitored by measuring the transmembrane resistance using a Millicell-ERS apparatus (Millipore, Bedford, MA). After subtracting intrinsic resistance (filter alone without cell monolayers) from the total resistance, TEER was corrected for surface area and expressed as Ohms·cm^2 ($\Omega \cdot cm^2$). Only monolayers displaying TEER values above 198 $\Omega \cdot cm^2$ were used in the experiments. Transport studies were carried out with cell monolayers that were in culture for 21–25 days. For uptake studies, cells were seeded in six-well tissue culture plates (Falcon) with the same cell density. The entire medium was replaced every 2 days and 24 h before the start of each experiment. Monolayers were kept at 37°C, 5% CO_2, and 90% relative humidity.

On *days 21* to *23* after seeding, the medium was replaced with EMEM plus 1 mM AICAR (or EMEM alone for controls) in either the apical or basolateral or in both compartments. After incubation for the time specified (see RESULTS for details), transport was assessed at apical pH 5.5 by cell uptake and transepithelial flux studies of the radiolabeled neutral dipeptide [^{3}H]-D-Phe-L-Gln.

The monolayers were washed twice with warm Krebs solution, pH 7.4 (containing 10 mM glucose). After being washed, they were preincubated at 37°C for 30 min, and TEER was recorded. The Krebs solution on both sides of the cell monolayers was then removed by aspiration. For the measurement of apical entry as well as for apical to basolateral transport, 250 μl of fresh Krebs (pH 5.5) containing 0.42 μM [^{3}H]-D-Phe-L-Gln was added on the apical side and 600 μl of Krebs (pH 7.4) on the basolateral side of cells that were either preincubated with 1 mM AICAR in EMEM for 24 h or to control cells treated with EMEM alone. The monolayers were incubated at 37°C. Samples were taken from the basolateral compartment at 10, 20, and 30 min followed by an immediate replacement of the same volume of fresh Krebs solution (pH 7.4, 37°C). The samples taken from the basolateral compartment were then placed in vials, and their radioactive content was determined via scintillation counting [Aqueous Counting Scintillant (ACS II), Amersham Biosciences, Piscataway, NJ]. At 30 min, Krebs from both sides of the monolayer was aspirated, cells were washed three times in fresh cold Krebs (pH 7.4, 4°C), filters were removed and placed in vials similarly as described above, and radioactive content was determined via scintillation counting. For the measurement of the peptide basolateral entry, 600 μl of fresh Krebs (pH 7.4) containing 0.42 μM [^{3}H]-D-Phe-L-Gln was added on the basolateral side, and filters were similarly processed as described above.

As detailed above, the hPepT1-mediated transport of [^{3}H]-D-Phe-L-Gln into the Caco-2 cell monolayer and the mediated transepithelial rate have been calculated by subtraction of the transport observed in the presence of 20 mM Gly-L-Gln. In preliminary experiments using [^{14}C]-mannitol as a paracellular marker, it was shown that AICAR does not affect the rate of transport of this molecule (data not shown). Time course experiments showed that the apical to basolateral [^{3}H]-D-Phe-L-Gln flux was linear over 30 min (data not shown).

Measurement of intracellular pH by fluorimetry. Caco-2 cells were seeded onto glass cover slips cut to fit into 3-ml plastic cuvettes and allowed to grow to confluency for 10 days before the intracellular pH (pH_i) was measured using previously detailed methods (29). After being washed with PBS, the cells were incubated with BCECF-AM, the cell permeable ester form of the proton-sensitive fluoriprobe BCECF [2′,7′-bis-2-(carboxyethyl)−5(6)-carboxylfluorescein; Molecular Probes, Invitrogen, Paisley, UK; 10 μM for 20 min], and then rinsed with PBS. The cover slips were put in a plastic cuvette containing Krebs solution (pH 5.5) and placed in a spectrofluorometer (Hitachi; excitation wavelength alternating between 439 and 490 nm, emission wavelength 535 nm) with a thermostatically regulated cuvette holder (37°C). The 490/439-nm ratio was calibrated using the nigericin (2 μM)/high potassium method of Thomas et al. (26), which also confirmed that the fluorimetric assay was working.

Immunogold electron microscopy. Control and AICAR-treated Caco-2 cells grown on polyester filters were prepared for immunogold electron microscopy (EM) by standard methods (3). Briefly, filters were stained with osmium and uranyl acetate (2% wt/vol in distilled water), dehydrated through increasing concentrations of ethanol (70–100%), and embedded in Spur resin (Agar, Reading, UK). Ultrathin

sections (50–80 nm) were prepared by use of a Reichert Ultracut S ultratome (Leica, Milton Keynes, UK), mounted on 200-mesh nickel grids, incubated at room temperature with either anti-PepT1 antibody (14, 21) (dilution 1:200, 2 h), and then anti-rabbit 15-nm gold complex (British Biocell, Cardiff, UK; 1:60, 1 h), or anti-glucose transporter 2 (GLUT2) antibody [Santa Cruz Biotechnology GLUT2 (E15) antibody; Insight Biotechnology, Wembley, UK; 1:200, 2 h], and then anti-goat 5-nm gold complex (British Biocell; 1:60, 1 h). All antisera were diluted in 0.1 M phosphate buffer containing 0.1% egg albumin. As a negative control, the primary antibody was replaced by nonimmune rabbit sera and immunogold labeling was not observed. After immunolabeling sections were lightly counterstained with lead citrate and uranyl acetate and examined with a JEOL transmission electron microscope (JEM-1010; JEOL, Peabody, MA), and representative micrographs were prepared. The area of the cells was determined by point-counting morphometry, and the number of gold particles was counted. The density of immunogold (particles per μm^2) was then calculated for 8 cells per condition.

Statistical analysis. Data were expressed as means ± SE. When mentioned in the results, data are normalized to the control data and expressed as a ratio. Statistical analysis of data was assessed by Student's *t*-test, or by one-way ANOVA, P values of <0.05 were considered statistically significant.

RESULTS

Uptake of [^{3}H]-D-Phe-L-Gln cellular uptake was significantly decreased in AICAR-treated Caco-2 cells. To initially establish whether AICAR had an effect on hPepT1-mediated [^{3}H]-D-Phe-L-Gln uptake, Caco-2 cells were cultured in six-well plates for 10 days before pretreatment for 24 h with 1 mM AICAR. As can be seen in Fig. 1, there was a significant decrease in the hPepT1-mediated uptake of the dipeptide after AICAR pretreatment (132 ± 5.1 fmol·cm^{-2}·60 min^{-1} vs. control 222 ± 10.7 fmol·cm^{-2}·60 min^{-1}, $P < 0.05$, without any decrease in total protein in the wells).

AICAR treatment (1 mM) for 24 h activates AMPK in Caco-2 monolayers grown on solid plastic. AMPK is known to activate acetyl-CoA carboxylase by phosphorylation at residue Ser79. Western blotting demonstrated an increase in the Ser79-phosphorylated form of acetyl-CoA carboxylase (Fig. 1), confirming that AICAR was activating AMPK, in agreement with previous studies (for example, see Refs. 22 and 28).

Apical [^{3}H]-D-Phe-L-Gln cellular uptake was significantly decreased in AICAR-treated Caco-2 monolayers on Transwell filters. Pretreatment of the cells for 24 h with 1 mM AICAR resulted in significantly decreased hPepT1-mediated [^{3}H]-D-Phe-L-Gln apical influx compared with control cells (291 ± 29 vs. 490 ± 30 fmol·cm^{-2}·30 min^{-1}, respectively, $P < 0.05$, Fig. 2*A*). AICAR treatment had no effect on nonmediated cell influx (i.e., that not inhibited in the presence of 20 mM Gly-L-Gln, for example, 152 ± 18 vs. 159 ± 37 fmol·cm^{-2}·30 min^{-1} control vs. AICAR-treated, respectively; one representative experiment, $n = 4$ filters per condition, where mediated uptake under control conditions was 451 ± 49 fmol·cm^{-2}·30 min^{-1}).

A time course of the AICAR-induced reduction in apical [^{3}H]-D-Phe-L-Gln uptake into Caco-2 cells grown on Transwell filters indicated that, although there was a trend toward reduction in uptake at 2 h, this did not always reach statistical significance; a significant reduction was usually established after 4 h, and this effect was sustained at the same level until 24 h (data not shown). TEER values were compared for control and cells treated with 1 mM AICAR for 24 h to check whether 24-h exposure to AICAR was exhibiting any toxic effects. Mean TEER values were significantly increased after 24-h AICAR treatment (248 ± 9 vs. 293 ± 5 Ω·cm^2 for control and treated cells respectively, $P < 0.001$), as is consistent with other cell types (see DISCUSSION) and indicating that there was no loss of cell viability.

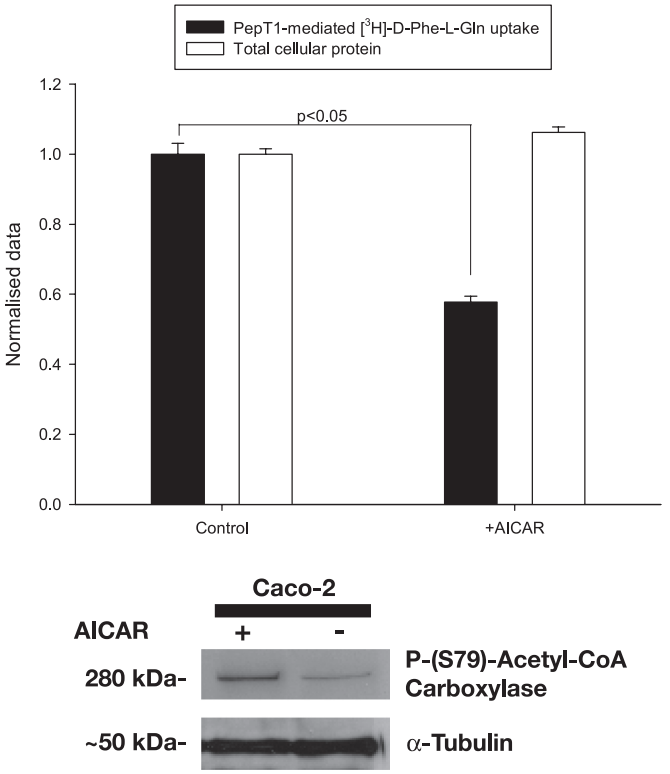

Fig. 1. *Top*: mediated [^{3}H]-D-Phe-L-Gln uptake into Caco-2 cells grown on 6-well plates. [^{3}H]-D-Phe-L-Gln-mediated cell influx in cells grown on 6-well plates for 10 days is significantly reduced when treated with 1 mM 5-amino-imidazole-4-carboxamide-ribonucleoside (AICAR) for 24 h compared with control cells (solid bars). Total cellular protein was not altered treated with 1 mM AICAR for 24 h (compared to control cells) as determined by Bradford protein assay (open bars). The data are normalized to control uptake and control total protein and presented as mean ± SEM of the ratios between the treated and control cells. $P < 0.05$, $n = 5$ separate experiments, 4 wells per condition. The normalized value of control cellular uptake corresponds to 222 ± 11 fmol·cm^{-2}·60 min^{-1}, and the normalized value of control total cellular protein was 425 ± 5 μg. *Bottom*: Western blot demonstrating that AICAR activated AMP-activated protein kinase (AMPK) in Caco-2 cells. Treatment of a Caco-2 cell monolayer grown on sold plastic with 1 mM AICAR for 24 h resulted in an increase in the activated (Ser79 phosphorylated) form of acetyl-CoA carboxylase, a downstream target of AMPK.

Concentration dependence of AICAR on apical [^{3}H]-D-Phe-L-Gln uptake into Caco-2 cells grown on Transwell filters. Previous studies on membrane transporters (28) used AICAR at a concentration of 2.5 mM. Figure 2*B* shows that, when measuring hPepT1-mediated apical [^{3}H]-D-Phe-L-Gln uptake into Caco-2 cells grown on Transwell filters, the largest response was seen with 3.33 mM; however, at this concentration the monolayers had a tendency to lift off the filter (as shown by a decrease in TEER), so 1 mM was chosen as the best balance of effect and monolayer stability for all experiments.

Basolateral [^{3}H]-D-Phe-L-Gln cellular uptake was not affected by AICAR treatment of cells on Transwell filters. Direct measurement of the mediated cell influx via the basolateral

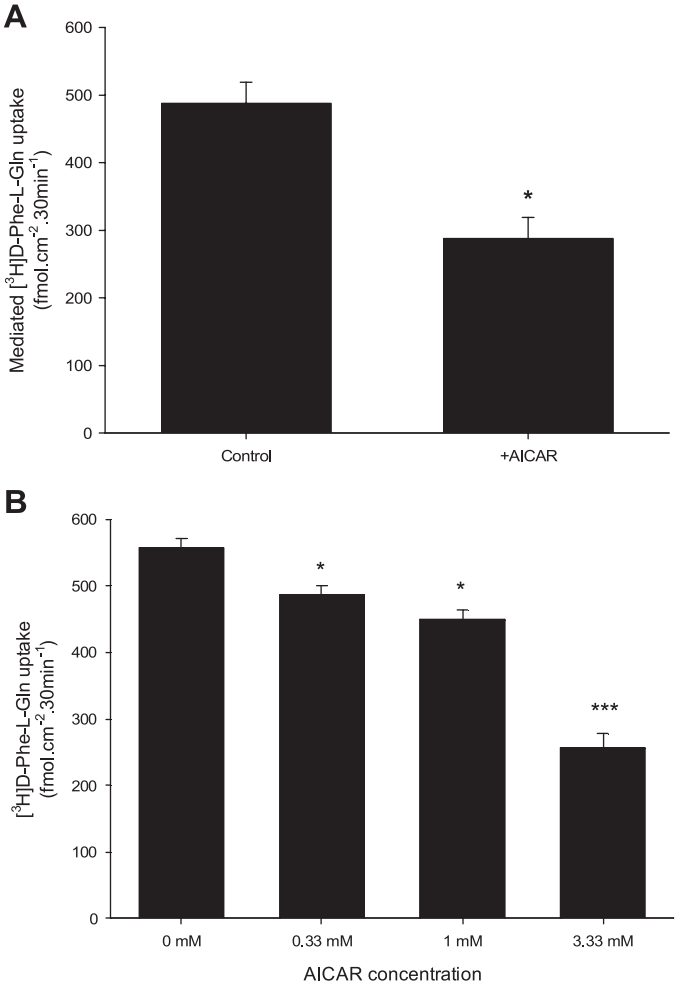

Fig. 2. *A*: apical [^{3}H]-D-Phe-L-Gln cellular uptake into Caco-2 monolayers grown on Transwell filters treated with 1 mM AICAR for 24 h compared with controls. Pretreatment of the cells for 24 h with 1 mM AICAR both apically and basolaterally resulted in significantly decreased PepT1-mediated [^{3}H]-D-Phe-L-Gln apical influx compared with control cells, (*$P < 0.05$, 1-way ANOVA, $n = 5$ separate experiments, 4 filters per experiment. Results are presented as peptide uptake in fmol·cm^{-2}·30 min^{-1}). *B*: apical [^{3}H]-D-Phe-L-Gln cellular uptake into Caco-2 monolayers on Transwell filters treated with increasing concentrations of AICAR. Treatment with both 0.33 mM and 1 mM AICAR concentrations for 24 h resulted in significantly decreased PepT1-mediated apical peptide influx compared with controls, with results being more consistent when 1 mM AICAR was used (*$P < 0.05$, ***$P < 0.001$, 1-way ANOVA, $n = 4$ filters, 1 representative experiment. Results are presented as peptide uptake in fmol·cm^{-2}·30 min^{-1}). At 3.33 mM AICAR displays additional effects as the monolayers are disrupted (indicated by a drop in transepithelial electrical resistance, TEER, values; data not shown). Therefore AICAR was subsequently used at concentration of 1 mM.

membrane of Caco-2 cell monolayers grown on filters displayed no significant alteration following AICAR treatment (1 mM for 24 h, AICAR 67.1 ± 7 fmol·cm^{-2}·30 min^{-1} vs. controls 87.5 ± 12 fmol·cm^{-2}·30 min^{-1}, $P > 0.05$).

Apical-to-basolateral-mediated transepithelial flux of [^{3}H]-D-Phe-L-Gln was not reduced in AICAR-treated Caco-2 cell monolayers on Transwell filters. From the previous experiments apical cell entry was shown to be reduced in the AICAR-treated cells; nevertheless in the same cells the mediated rate of [^{3}H]-D-Phe-L-Gln apical-to-basolateral transepithelial flux was not reduced. Pretreatment of the cells for 24 h with 1 mM AICAR did not significantly reduce the mediated rate of apical to basal flux (6.2 ± 1.4 vs. control 4.1 ± 0.7 fmol·cm^{-2}·min^{-1}).

AICAR inhibition of apical cell uptake through hPepT1 remained in the presence of S3226, an NHE3 inhibitor. To examine whether the decreased peptide influx observed in the treated cells is caused by an effect of AICAR on NHE3, peptide influx was measured as previously described (23) in the presence and absence of AICAR (1 mM, 24 h) and in the presence or absence of the specific NHE3 inhibitor, S3226 added acutely.

Results presented in Fig. 3 illustrate that, although blocking of NHE3 by acute addition of 10 μM S3226 to the apical compartment of Transwell filters caused a clear reduction (122 ± 10 fmol·cm^{-2}·30 min^{-1} vs. controls 177 ± 9 fmol·cm^{-2}·30 min^{-1},$P < 0.05$) in the mediated peptide influx (in agreement with Ref. 18), the inhibitory effect of AICAR was still evident. Thus, in cells pretreated for 24 h with 1 mM AICAR where the NHE3 exchanger was also acutely blocked, further significant inhibition of mediated transport was evident (65 ± 13 fmol·cm^{-2}·30 min^{-1} vs. control 122 ± 10 fmol·cm^{-2}·30 min^{-1}, $P < 0.05$). These results imply that the AICAR inhibitory effect is additive to that of S3226 and thus not directly linked to the NHE3 protein. For these experiments the apical pH was adjusted to 6.5 because this had previously been shown to be the most appropriate value for studying the effect of NHE3 on peptide transport (18).

The effect of AICAR on Caco-2 pH$_i$ as measured by fluorimetry. To determine whether the proton-driving force for peptide uptake had been affected by AICAR treatment, the pH$_i$ of Caco-2 cells grown on cover slips was measured by fluorimetry using the pH-sensitive dye BCECF. There was a small

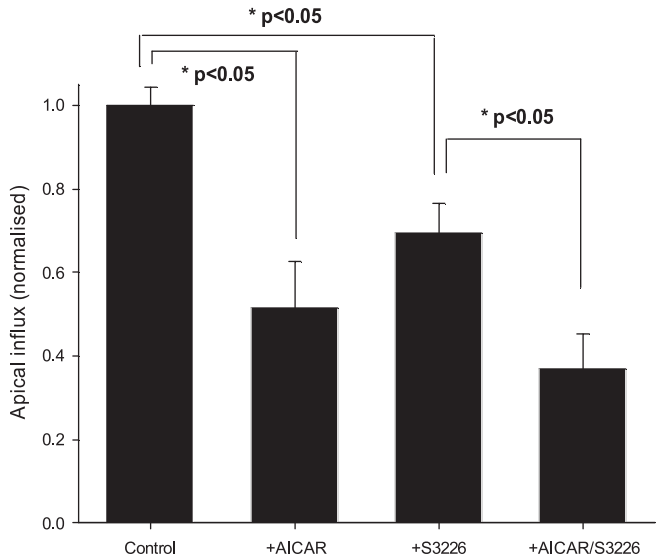

Fig. 3. AICAR effect in the presence of the specific sodium/hydrogen exchanger 3 (NHE3) inhibitor, S3226, on Caco-2 cells on Transwell filters. [^{3}H]-D-Phe-L-Gln mediated apical cell influx in control and cells pretreated for 24 h with 1 mM AICAR, grown on Transwell filters. S3226 (10 μl) was added acutely at time point $t = 0$ of the 30-min incubation time in both control and AICAR-treated cells. Nonmediated cell influx (in the presence of 20 mM Gly-L-Gln apically) has been subtracted from the data. The data are normalized to the control group (cellular uptake corresponds to 177 ± 9 fmol·cm^{-2}·30 min^{-1}; *$P < 0.05$, 1-way ANOVA, $n = 2$ separate experiments, 4 filters per experiment).

rise in pH_i after 1 mM AICAR treatment for 12 h (7.4 ± 0.07 to 7.73 ± 0.07, respectively, $P < 0.001$, $n = 3$), which should if anything increase the uptake of [^{3}H]-D-Phe-L-Gln through hPepT1.

In addition, changes in transport cannot be accounted for by an effect of AICAR on cell volume, as this was determined by confocal microscopy and found to be the same between control and AICAR-treated cells (results not shown).

Immunogold EM of hPepT1 and GLUT2 in Caco-2 cell monolayers grown on Transwell filters. hPepT1 and GLUT2 protein expression was determined via immunogold EM (Fig. 4, PepT1 = arrows, GLUT2 = arrowheads). In the control Caco-2 cells, hPepT1 was shown to be largely at the brush-border (apical) membrane (Fig. 4*A*) with some intracellular staining (Fig. 4*C*). There was no hPepT1 at the basolateral membrane (Fig. 4*E*), unlike for GLUT2. In agreement with the literature (reviewed in Ref. 17), GLUT2 was found at the apical membrane of the Caco-2 monolayer, as well as intracellularly (Fig. 4, *A* and *C*, respectively). The quantified data are presented in Fig. 5.

Brush-border membrane-bound hPepT1 was shown to be significantly reduced in the monolayers treated with 1 mM AICAR for 12 h (0.17 ± 0.01 gold particles per μm^2), compared with controls (0.36 ± 0.03 gold particles per μm^2, $P < 0.001$; Fig. 4, *B* and *A*, respectively). Cytoplasmic hPepT1 immunoreactivity in contrast was significantly increased for the AICAR-treated cells (0.31 ± 0.03 gold particles per μm^2) compared with the controls (0.22 ± 0.03 gold particles per

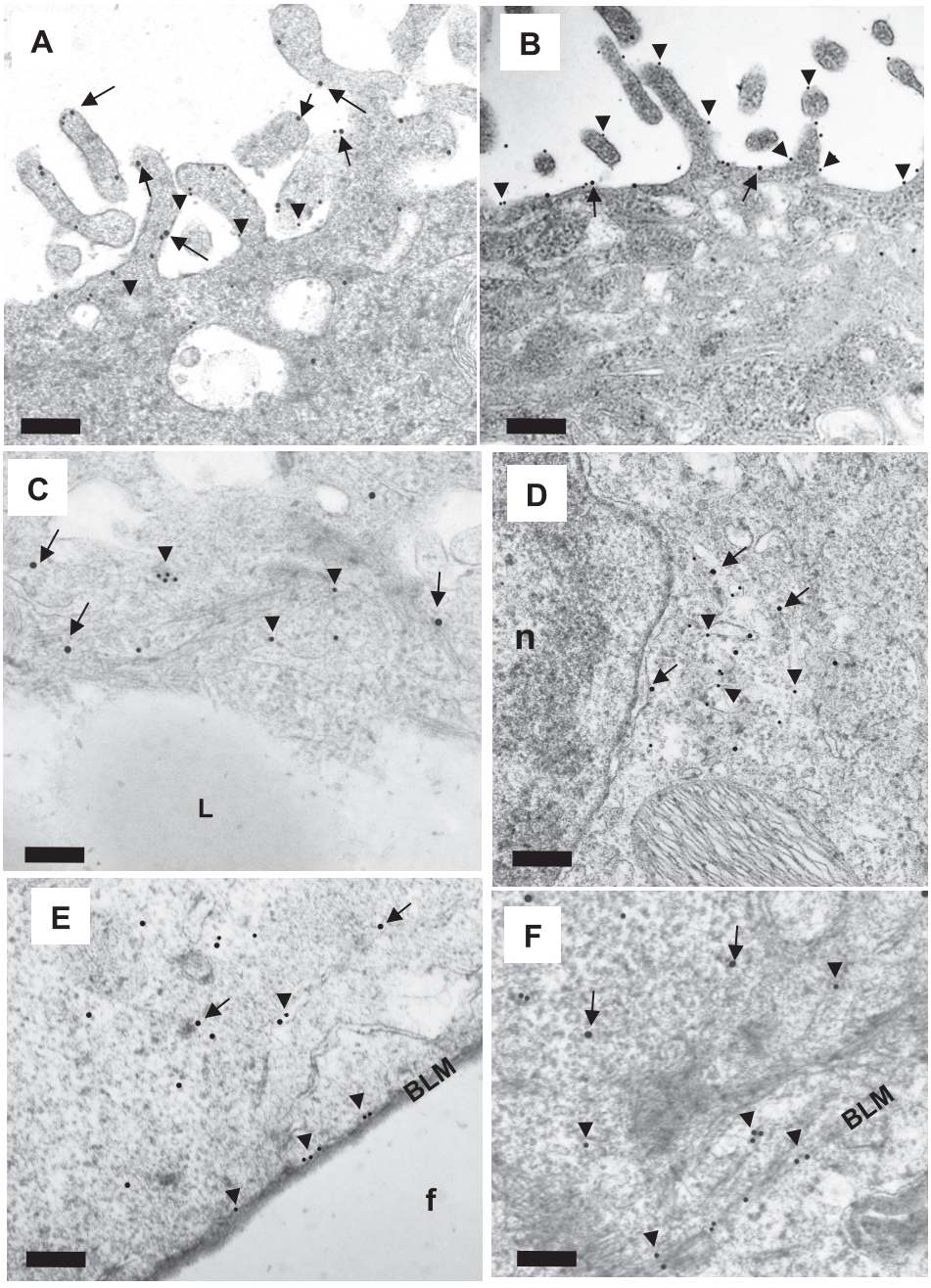

Fig. 4. Electron micrographs illustrating coimmunogold detection of hPepT1 and glucose transporter 2 (GLUT2) immunogold staining in Caco-2 cells grown on Transwell filters. The micrographs show representative images of brush border (*A* and *B*), cytosol (*C* and *D*), and basolateral membrane (BLM) (*E* and *F*) labeling. Control cells are shown in *A*, *C*, and *E*, and 1 mM AICAR -treated cells are shown in *B*, *D*, and *F*. Arrows indicate immunogold labeling of hPepT1, arrowheads GLUT2. Scale bar represents 200 nM, n, nucleus; f, filter; L, lipid droplet.

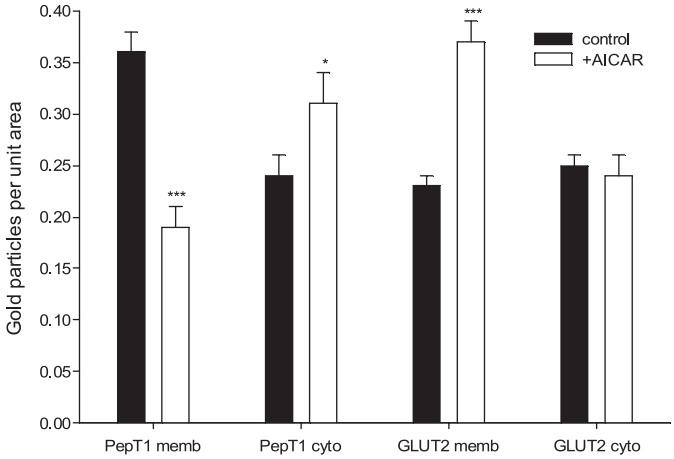

Fig. 5. Quantification of hPepT1 and GLUT2 transporters in Caco-2 cell monolayers on Transwell filters using immunogold electron microscopy. Quantification of gold particles in control (solid bars) and with 1 mM AICAR treatment for 12 h (open bars) for hPepT1 and GLUT2 in the brush-border membrane (PepT1 memb and GLUT2 memb, respectively) and in the cytoplasm (PepT1 cyto and GLUT2 cyto, respectively). $*P < 0.05$, $***P < 0.001$ compared with relevant control value.

μm^2) (Fig. 4, *D* and *C*, respectively), while again hPepT1 was not discernible at the basolateral membrane (Fig. 4*F*). Consequently, total immunoreactivity (brush-border membrane plus cytoplasm) remained constant between treated and control cells (Fig. 5).

The opposite result was seen for the facilitated glucose transporter GLUT2 (Fig. 4, *B*, *D*, and *F* and Fig. 5), in that brush-border membrane-bound transporter was significantly increased after AICAR pretreatment (from 0.23 ± 0.01 to 0.37 ± 0.02 gold particles per μm^2, $P < 0.001$) although for GLUT2 there was no significant loss of immunoreactivity from the cytoplasm. Both of these findings for GLUT2 are in agreement with the findings of Ref. 28.

AICAR induced changes in Caco-2 cell monolayer morphology. When the sections used to quantify the immunogold staining were imaged at low magnification, changes in the morphology of the apical membrane of the Caco-2 cells treated with 1 mM AICAR for 12 h were observed with an almost complete loss of the apical microvilli structures (Fig. 6).

DISCUSSION

In the present study, we have demonstrated that peptide uptake in the small intestine model cell line Caco-2 is altered when cells are incubated with the AMPK activator, AICAR. The metabolic-sensing kinase, AMPK, has emerged recently as an important sensor and regulator of a variety of cellular processes, which act to generate ATP levels in the stressed cell (9). Under conditions of metabolic stress, the expression and activity of many membrane-transport proteins are inhibited, thereby limiting the dissipation of transcellular ionic gradients and preserving the cellular energy required to maintain them. A growing number of studies suggest that AMPK modulates the activities of several important membrane-transport proteins (8). To date, however, the underlying mechanisms involved in metabolism-transport coupling have not been well defined.

The maintenance of transmembrane ion and solute gradients is required for normal cellular function, viability, and coordinated transepithelial transport, but it also consumes a substantial portion of total cellular energy. Peptide absorption in the intestinal epithelium is an energy-dependent process because the proton force that drives peptide uptake through PepT1 is maintained by the apical sodium-hydrogen exchanger NHE3 (18), whose activity is in turn dependent on the Na/K-ATPase on the basolateral membrane, i.e., PepT1 is a tertiary active transport system. It is no different in the Caco-2 cell system, where peptide influx across the apical cell membrane is achieved via the H^+/coupled peptide transporter, hPepT1. A basolateral peptide transporter has also been functionally shown to be present in Caco-2 cells, and studies so far demonstrate that it is an energy-independent process (25) and appears subject to regulation (11). Results presented in this study strongly support the hypothesis that the energy-consuming apical peptide uptake is inhibited in the energy-depleted cell, whereas the basolateral facilitated system is upregulated, linking peptide transport directly to the cellular metabolic state.

Cellular apical peptide transport was found to be significantly reduced in the AICAR-treated cells. This was evident in

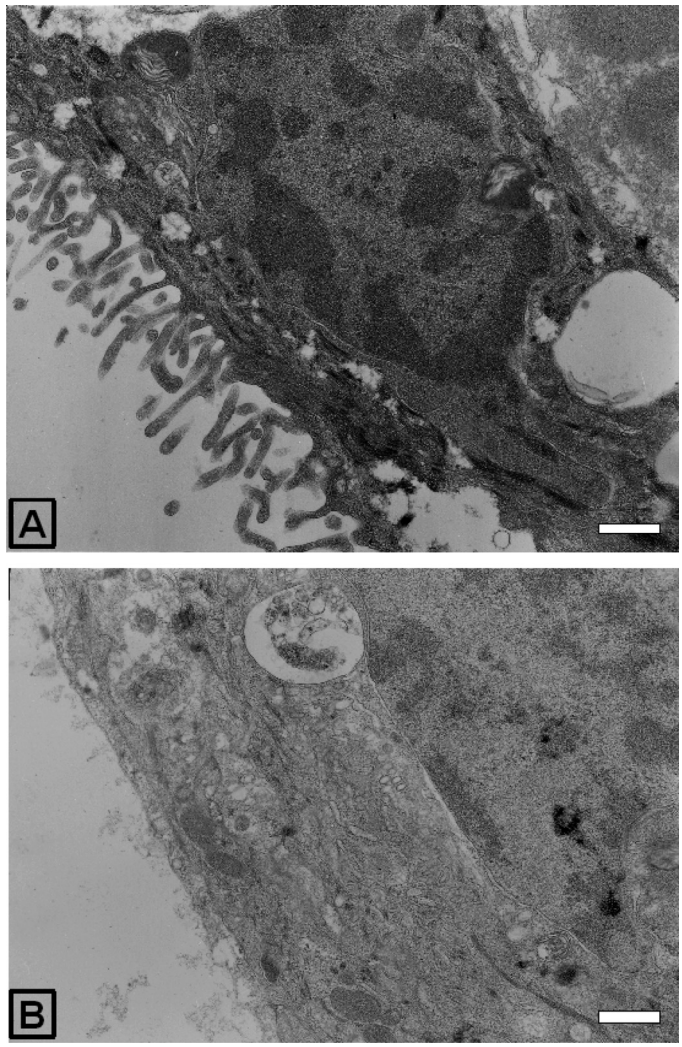

Fig. 6. Structural changes in Caco-2 cell monolayers on Transwell filters determined by electron microscopy. Electron micrographs of Caco-2 cells in Transwell filters at ×12,000 magnification, control (*A*), and after 12-h 1 mM AICAR treatment (*B*). Scale bar represents 500 nm.

cells grown on plates as well as cells grown on permeable supports when both sides of the cell monolayer are treated with AICAR. Despite the reduced peptide uptake in the AICAR-treated cells grown on six-well plates, total protein determination showed no differences between treated and untreated wells, suggesting that this effect was not attributable to a reduction in the number of cells. The decrease in PepT1-mediated uptake across the apical membrane could not be attributed to a decrease in the proton gradient, as measurements of the pH_i of the cells showed that pH_i rose slightly after AICAR treatment, which would in fact, if anything, increase the driving force with the extracellular pH buffered to pH 5.5 in the experiments. Consistent with this is the observation that the AICAR effect was additive to that of the NHE3 inhibitor S3226.

A surprising result was that apical-to-basolateral transepithelial flux (involving additionally the basolateral peptide transporter) was not altered in the AICAR-treated monolayers; if anything the trend appeared to be for an increase in flux (albeit not statistically significant). As the cell volume did not change in the presence of AICAR, the reduced apical influx of peptide would have lead to a reduced intracellular concentration. The concentration of dipeptide used in these transport experiments were submicromolar, and the basolateral peptide transporter has been reported to be of relatively low (millimolar) affinity (25), so the efflux rate across the basolateral membrane would be expected to be directly proportional to the intracellular peptide concentration. Therefore, to maintain transepithelial flux in the AICAR-treated monolayers, there must have been a reciprocal upregulation of the activity of the basolateral peptide transport system in the Caco-2 cells.

Increased paracellular permeability of the monolayer was not the cause of these observations, as TEER data showed increased tight junction resistance in monolayers treated with AICAR. This confirms previous studies that have shown effects of AICAR on TEER and the tight junction properties of other epithelial cell lines (6, 12, 31). For example, it has previously been shown that, in polarized Madin-Darby canine kidney (MDCK) cells, AICAR promotes transepithelial resistance development and tight junction assembly upon switching calcium from low to normal concentrations (31) via activation by the protein kinase LKB1. Results presented in this study show that, in Caco-2 cell monolayers, AICAR incubation for up to 24 h exhibited a similar effect because TEER values were significantly increased in the treated cells. Despite the confirmation of this phenomenon by the observations made here, the mechanism behind these results still remains to be elucidated.

In agreement with the reduced apical peptide intake, immunogold EM localization of hPepT1 showed that, in the presence of AICAR, hPepT1 was significantly reduced in the apical brush-border membrane. hPepT1 was not detected in the basolateral membrane. Additionally, because after AICAR treatment the total amount of hPepT1 immunoreactivity (i.e., brush-border plus intracellular) was not reduced, this is suggestive of regulation via trafficking rather than transcription/translation or posttranscriptional modification, as hPepT1 does not possess AMPK phosphorylation sites on the basis of the reported consensus motif for AMPK phosphorylation (10). The effect of AICAR on the basolateral transporter is more difficult to interpret because we presently have no information about its molecular identity.

The striking reduction in the number of microvilli at the apical brush-border seen after AICAR treatment (best illustrated in the lower magnification electron micrographs, Fig. 6) is reported here for the first time to our knowledge. In most studies using AICAR, the amount of brush-border protein is assayed using surface protein biotinylation followed by Western blotting, e.g., with intestinal GLUT2 (28), and thus changes in the structure of the cells would not be seen. It is unlikely that the changes in the apical membrane that we see are simply attributable to a toxic effect of the AICAR treatment for several reasons. First, the monolayers become tighter (TEER data); second, the cells become less permeable to apical dipeptide; and third, and in our view most convincingly, in the same cells the apical levels of GLUT2 increased (as seen in Ref. 28). Thus there is a reciprocal regulation of PepT1 and GLUT2 as predicted by the role of AMPK in reducing cell energy expenditure. Interestingly, reciprocal regulation of PepT1 and GLUT2 has been recently reported in the small intestine, mediated by calcium and protein kinase C βII (19). Intriguingly, activation of the protein kinase LKB1, which in turn activates AMPK, causes the polarization of single cells of modified colonic epithelial cell lines by remodeling their actin cytoskeleton into a brush border and reorganizing their tight junction complexes (2). LKB1 is a tumor suppressor gene (Peutz-Jeghers Syndrome patients with mutations in LKB1 suffer from gastrointestinal tumors) and is also implicated in cell energy regulation (reviewed in 1). The increase in the "tightness" of tight junctions and the polarization, along with the activation of p53 and induction of cell cycle arrest (16) and inactivation of mTOR (15, 24), are ways in which AMPK is thought to have an antiproliferative effect (31). AICAR treatment in our Caco-2 cell experiments resulted in an increase in tight junction resistance but a loss of polarization (as assessed by a loss of the brush-border microvilli). However, LKB1 activation affects another thirteen downstream kinases in addition to AMPK (1), and it has been reported in MDCK cells that AMPK cannot mediate all of the effects of LKB1 activation (31), which may potentially explain the discrepancy between LKB1 and AMPK activation.

In summary, it is known that, in conditions of metabolic stress, activation of AMPK results in a shift of glucose uptake from sodium-dependent sodium-glucose transporters to the sodium-independent GLUT class (28). Our findings for peptide transport are conceptually identical, in that the activity of the energy-dependent apical peptide transporter hPepT1 is reduced while the transepithelial flux of our model hydrolysis-resistant dipeptide is maintained, presumably by an increase in the basolateral permeability. Understanding these changes in the activity of different membrane transporters will be of importance if such transporters are the route of uptake of anticancer (pro)drugs, as cells in solid tumors are likely to be metabolically stressed (by hypoxia and/or glucose deprivation), and this may therefore affect the efficacy of treatment.

ACKNOWLEDGMENTS

We thank the following from the Department of Physiology, Anatomy & Genetics, University of Oxford: Lynne Scott for immunogold EM sample preparation; George Trichas for help determining Caco-2 cell volume; Dr. Siobhan Moyes for Caco-2 cells and helpful discussion. We are very grateful to Miss Sabine Heublein for technical expertise in performing the Western blot.

GRANTS

This study was supported by The Wellcome Trust and Cancer Research UK.

DISCLOSURES

No conflicts of interest, financial or otherwise, are declared by the author(s).

REFERENCES

1. **Alessi DR, Sakamoto K, Bayascas JR.** LKB1-dependent signaling pathways. *Annu Rev Biochem* 75: 137–163, 2006.
2. **Baas AF, Kuipers J, van der Wel NN, Batlle E, Koerten HK, Peters PJ, Clevers HC.** Complete polarization of single intestinal epithelial cells upon activation of LKB1 by STRAD. *Cell* 116: 457–466, 2004.
3. **Christian HC, Taylor AD, Flower RJ, Morris JF, Buckingham JC.** Characterization and localization of lipocortin 1-binding sites on rat anterior pituitary cells by fluorescence-activated cell analysis/sorting and electron microscopy. *Endocrinology* 138: 5341–5351, 1997.
4. **Corton JM, Gillespie JG, Hawley SA, Hardie DG.** 5-aminoimidazole-4-carboxamide ribonucleoside. A specific method for activating AMP-activated protein kinase in intact cells? *Eur J Biochem* 229: 558–565, 1995.
5. **Daniel H.** Molecular and integrative physiology of intestinal peptide transport. *Annu Rev Physiol* 66: 361–384, 2004.
6. **Forcet C, Billaud M.** Dialogue between LKB1 and AMPK: a hot topic at the cellular pole. *Sci STKE* 2007: pe51, 2007.
7. **Ganapathy ME, Brandsch M, Prasad PD, Ganapathy V, Leibach FH.** Differential recognition of beta -lactam antibiotics by intestinal and renal peptide transporters, PEPT 1 and PEPT 2. *J Biol Chem* 270: 25672–25677, 1995.
8. **Hallows KR.** Emerging role of AMP-activated protein kinase in coupling membrane transport to cellular metabolism. *Curr Opin Nephrol Hypertens* 14: 464–471, 2005.
9. **Hardie DG.** New roles for the LKB1-AMPK pathway. *Curr Opin Cell Biol* 17: 167–173, 2005.
10. **Hardie DG, Scott JW, Pan DA, Hudson ER.** Management of cellular energy by the AMP-activated protein kinase system. *FEBS Lett* 546: 113–120, 2003.
11. **Henderson FD, Ayrton A, Simmons NL, Thwaites DT.** cAMP dependent regulations of basolateral glycyl-sarcosone uptake by human intestinal Caco-2 cell monolayers. *J Physiol* 549P: PC9, 2003.
12. **Hezel AF, Gurumurthy S, Granot Z, Swisa A, Chu GC, Bailey G, Dor Y, Bardeesy N, Depinho RA.** Pancreatic LKB1 deletion leads to acinar polarity defects and cystic neoplasms. *Mol Cell Biol* 28: 2414–2425, 2008.
13. **Hidalgo IJ, Raub TJ, Borchardt RT.** Characterization of the human colon carcinoma cell line (Caco-2) as a model system for intestinal epithelial permeability. *Gastroenterology* 96: 736–749, 1989.
14. **Hussain I, Kellett L, Affleck J, Shepherd J, Boyd R.** Expression and cellular distribution during development of the peptide transporter (PepT1) in the small intestinal epithelium of the rat. *Cell Tissue Res* 307: 139–142, 2002.
15. **Inoki K, Zhu T, Guan KL.** TSC2 mediates cellular energy response to control cell growth and survival. *Cell* 115: 577–590, 2003.
16. **Jones RG, Plas DR, Kubek S, Buzzai M, Mu J, Xu Y, Birnbaum MJ, Thompson CB.** AMP-activated protein kinase induces a p53-dependent metabolic checkpoint. *Mol Cell* 18: 283–293, 2005.
17. **Kellett GL, Brot-Laroche E, Mace OJ, Leturque A.** Sugar absorption in the intestine: the role of GLUT2. *Annu Rev Nutr* 28: 35–54, 2008.
18. **Kennedy DJ, Leibach FH, Ganapathy V, Thwaites DT.** Optimal absorptive transport of the dipeptide glycylsarcosine is dependent on functional Na+/H+ exchange activity. *Pflügers Arch* 445: 139–146, 2002.
19. **Mace OJ, Lister N, Morgan E, Shepherd E, Affleck J, Helliwell P, Bronk JR, Kellett GL, Meredith D, Boyd R, Pieri M, Bailey PD, Pettcrew R, Foley D.** An energy supply network of nutrient absorption coordinated by calcium and T1R taste receptors in rat small intestine. *J Physiol* 587: 195–210, 2009.
20. **Meredith D.** Site-directed mutation of arginine 282 to glutamate uncouples the movement of peptides and protons by the rabbit proton-peptide cotransporter PepT1. *J Biol Chem* 279: 15795–15798, 2004.
21. **Panitsas KE, Boyd CA, Meredith D.** Evidence that the rabbit proton-peptide co-transporter PepT1 is a multimer when expressed in Xenopus laevis oocytes. *Pflügers Arch* 452: 53–63, 2006.
22. **Peng L, Li ZR, Green RS, Holzman IR, Lin J.** Butyrate enhances the intestinal barrier by facilitating tight junction assembly via activation of AMP-activated protein kinase in Caco-2 cell monolayers. *J Nutr* 139: 1619–1625, 2009.
23. **Schwark JR, Jansen HW, Lang HJ, Krick W, Burckhardt G, Hropot M.** S3226, a novel inhibitor of Na+/H+ exchanger subtype 3 in various cell types. *Pflügers Arch* 436: 797–800, 1998.
24. **Shaw RJ, Bardeesy N, Manning BD, Lopez L, Kosmatka M, DePinho RA, Cantley LC.** The LKB1 tumor suppressor negatively regulates mTOR signaling. *Cancer Cell* 6: 91–99, 2004.
25. **Terada T, Sawada K, Saito H, Hashimoto Y, Inui K.** Functional characteristics of basolateral peptide transporter in the human intestinal cell line Caco-2. *Am J Physiol Gastrointest Liver Physiol* 276: G1435–G1441, 1999.
26. **Thomas JA, Buchsbaum RN, Zimniak A, Racker E.** Intracellular pH measurements in Ehrlich ascites tumor cells utilizing spectroscopic probes generated in situ. *Biochemistry* 18: 2210–2218, 1979.
27. **Thwaites DT, Brown CD, Hirst BH, Simmons NL.** Transepithelial glycylsarcosine transport in intestinal Caco-2 cells mediated by expression of H(+)-coupled carriers at both apical and basal membranes. *J Biol Chem* 268: 7640–7642, 1993.
28. **Walker J, Jijon HB, Diaz H, Salehi P, Churchill T, Madsen KL.** 5-aminoimidazole-4-carboxamide riboside (AICAR) enhances GLUT2-dependent jejunal glucose transport: a possible role for AMPK. *Biochem J* 385: 485–491, 2005.
29. **Wilkins RJ, Hall AC.** Measurement of intracellular pH in isolated bovine articular chondrocytes. *Exp Physiol* 77: 521–524, 1992.
30. **Young ME, Radda GK, Leighton B.** Activation of glycogen phosphorylase and glycogenolysis in rat skeletal muscle by AICAR—an activator of AMP-activated protein kinase. *FEBS Lett* 382: 43–47, 1996.
31. **Zheng B, Cantley LC.** Regulation of epithelial tight junction assembly and disassembly by AMP-activated protein kinase. *Proc Natl Acad Sci USA* 104: 819–822, 2007.